

Advanced Propulsion Integrated within Structure

a project presented to
The Faculty of the Department of Aerospace Engineering
San José State University

in partial fulfillment of the requirements for the degree

Master of Science in Aerospace Engineering (g)E E E N 3 1 0 6 3 1 7 e W 3 1 0

© 2022
Jack R. Gallagher
ALL RIGHTS RESERVED

Table of Contents

Abstract	iii
List of Tables	v
List of Figures	vi
List of Symbols	vii
1. Introduction	1
1.1 Motivation	1
1.2 Literature Review	1
1.3 Project Proposal	8
1.4 Methodology	8
2. CubeSat Design	9
2.1 Structure	9
2.2 Skeletal Structure	10
2.3 Propulsion	11
3. CubeSat Launcher	14
3.1 CubeSat Launcher	14
4. Communication	16
4.1 Antenna	16
5. Power System	18
5.1 Battery	18
5.2 Solar Panels	18
6. Analysis	20
6.1 Finite Element Analysis	20
6.2 Thrust Analysis	26
7. Conclusion	29
References	30
Appendix A	33

List of Tables

Table 6.1 - Nozzle and throat data.....	28
Table 6.2 - Equation results.....	28

List of Figures

Figure 1.1 - CubeSat arrangements.....	1
Figure 1.2 - Binder jetting.....	2
Figure 1.3 - Directed energy deposition.....	3
Figure 1.4 - Material extrusion.....	4

1. Introduction

1.1 Motivation

CubeSats are the current focus for space programs located at the edge of Earth's atmosphere or just beyond it. These miniature satellites reduce the funds necessary for organizations to place them into orbit and this makes space experiments more accessible. The cost of the launch is almost nonexistent since CubeSats can be taken to space on rockets that are already planned to launch into space [1]. Improvements to the design of these satellites are inevitable in the future since the low cost allows for multiple design iterations and testing. The current precedent for CubeSats is to have

Materials (ASTM), AM should be separated into seven different sections. These seven processes are binder jetting (BJ), directed energy deposition (DED), material extrusion (ME), material jetting (MJ), powder bed fusion (PBF), sheet lamination (SL), and vat photopolymerization (VP) [4].

BJ has a thin liquid binder that is released onto thin layers of powder that joins the material together [5]. This material created with this process is not suitable to be utilized in structural situations since the powder is bonded together with an adhesive. The mechanical layout for BJ is shown in Figure 1.2. This process is relatively quick and can be created using materials such as metals, polymers, or ceramics.

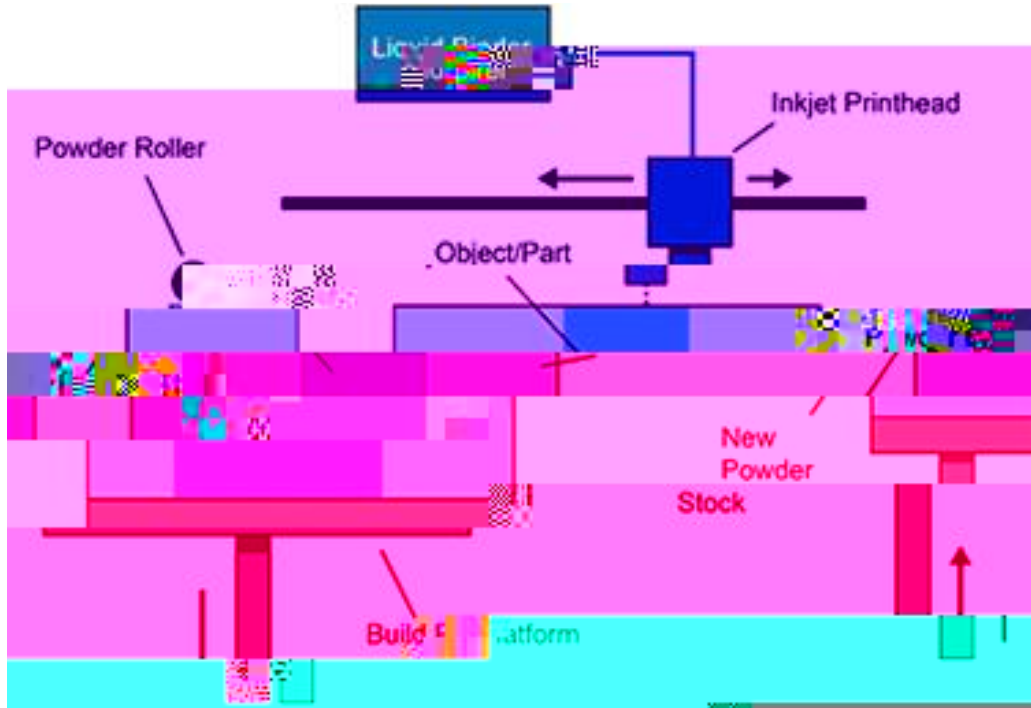


Figure 1.2 – Binder jetting [5].

DED deposits material that is then melted onto the surface of an already existing component. This process is only utilized to repair or add material to an already created part [6]. This process adds to the material layer by layer and this process is demonstrated in Figure 1.3. The only materials that are possible for this process are metals and this is because new material cannot be added to polymers or ceramics.

Figure 1.3 – Directed energy deposition [6].

ME has the material heated as it is pushed through a nozzle and then ejected onto a platform. This material is placed layer by layer to create the modeled component [7]. Figure 1.4 demonstrates the layout of the ME process. This process is only possible with the use of polymers and plastics as materials. The material fed through the nozzle needs to be constant during the whole process or the entire process will fail. The quality of this process is dependent on the size of the nozzle and the temperature of the material.

Figure 1.5 – Material jetting [8].

PBF utilizes a laser or electron beam that melts and fuses powdered material layer by layer. After a layer is completed, the platform is then lowered to allow for a powder to be rolled over the already completed section [9]. This allows for minute control over the design since the thinnest the material can be is the diameter of the heat source utilized. The setup is demonstrated in Figure 1.6. The main material used in PBF are metals, but polymers can be used as well.

Figure 1.6 – Powder bed fusion [9]sionng03(usi750.00000912 0 612 792 reW* nI

SL layers thin sheets of material onto one another and are then bonded together through ultrasonic welding as shown in Figure 1.7. After the welding of each layer, the shape and unbonded material are cut by a laser and this process is completed for each of the layers. The materials available for this process are any that could be rolled up such as plastic or some sheets of metal.

Figure 1.7 – Sheet 1

Figure 1.8 – Vat photopolymerization [11].

AM processes are already being implemented into current designs for CubeSats, but most are only focusing on the different systems of the CubeSat such as the structure, antenna, or mechanisms within the CubeSat.

In an article titled “Additively manufactured mirrors for CubeSats” written by Carolyn Atkins and associates, they demonstrate a UK Space Agency (UKSA) funded project that designs and manufactures AM mirrors that would fit within a 3U CubeSat chassis [12]. The authors are looking into using AM for mirrors since this would allow for a lightweight but optimized design.

Another article titled “An additive manufactured CubeSat mirror incorporating a novel circular lattice” by Robert Snell and associates, revises AM for mirrors on CubeSats as well but focuses on the use of a lattice integrated into the structure of the mirror. This lattice structure is designed to create a lightweight mirror that would then increase the design freedom [13]. The authors would then be able to experiment with designs that have not been possible to test before.

In “Selective Laser Melting of a 1U CubeSat structure. Design for Additive Manufacturing and assembly” written by Alberto Boschetto and associates, focuses solely on redesigning the structural subsystem for CubeSats. They are utilizing AM since this would give them access to design that would be otherwise unobtainable if subtractive manufacturing was utilized [14]. The

2. CubeSat Design

2.1 Structure

The Advanced Propulsion Integrated within Structure (APIS) CubeSat structure is designed to fit the 6U design of a

This method as well as the desired tolerance is only available with this method while utilizing the desired material.

2.2 Skeletal Structure

The surrounding structure for APIS is designed to add support for the inner components of it excluding the propulsion system. This additional material will be lightweight because of a lattice structure design that allows for less material utilized while being able to contain the inner components. A lightweight design is desired since APIS is designed to be as light as possible. This lattice will be similar to the two main faces of APIS while the smaller faces will be more open so specific inner components can be swapped as desired. Even though the faces will have less material than a solid face, there will be panels placed on each side to protect the inner components eoundib1 0u1(to)8(pro

2.3 Propulsion

The APIS CubeSat propulsion system will utilize cold gas which will propel the CubeSat using the pressurized propellant stored within the propulsion system. This simplifies the complexity of the propulsion system since there is no need to create thermal protection in the propulsion system from the heat that would be generated from combustion. The tanks for the propellant will be interchangeable tanks that will increase the reusability of the CubeSat for multiple missions. The exact number of these tanks is not decided yet but is going to be two to four total tanks. The propellant chosen for this propulsion system is CO₂.

The system is designed with sixteen thrusters to total a grouping of two on each corner of the structure. Each thruster is facing toward the center of the CubeSat with an angle of 45°. This number of thrusters is designed to allow the

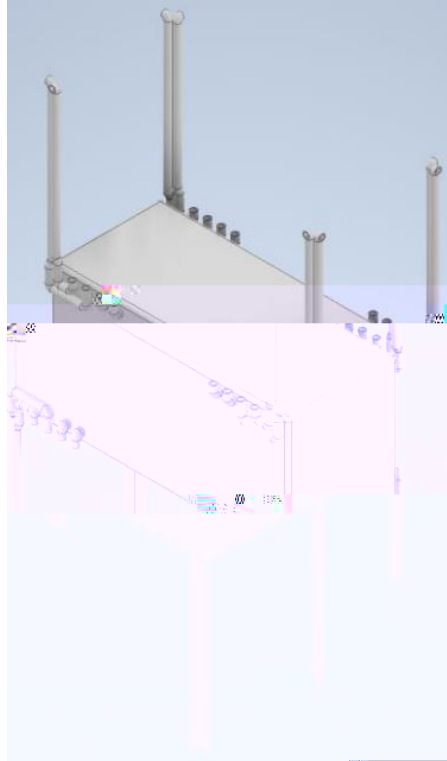


Figure 2.3 – Piping for the propulsion system.

The thrusters that are within the same corner of the structure will have a similar length for the propellant to travel within and each of the eight corners of the CubeSat will have the same piping path within each of them. Each corner of the CubeSat will have two thrusters with each being placed near the center of each of them. Since the piping is located within the support structure of the CubeSat, it does not interfere with the other compartments of the CubeSats and allows those spaces to be utilized to their max. This structure is only possible due to additive manufacturing processes because of the piping shown in Figure 2.3. This piping has intricate pathing that is impossible to complete in subtractive manufacturing due to it being within the structure.

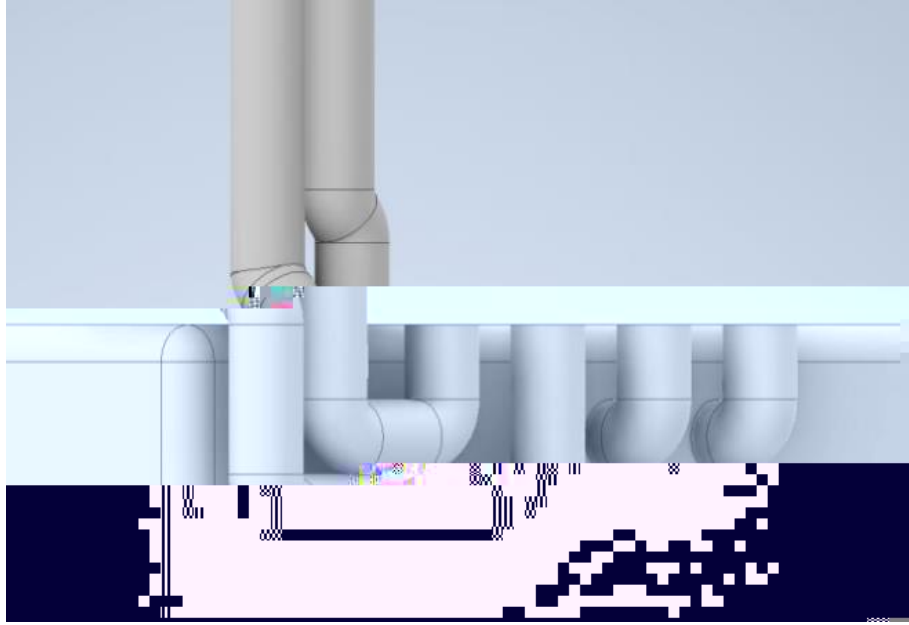


Figure 2.3 – Zoom in on piping.

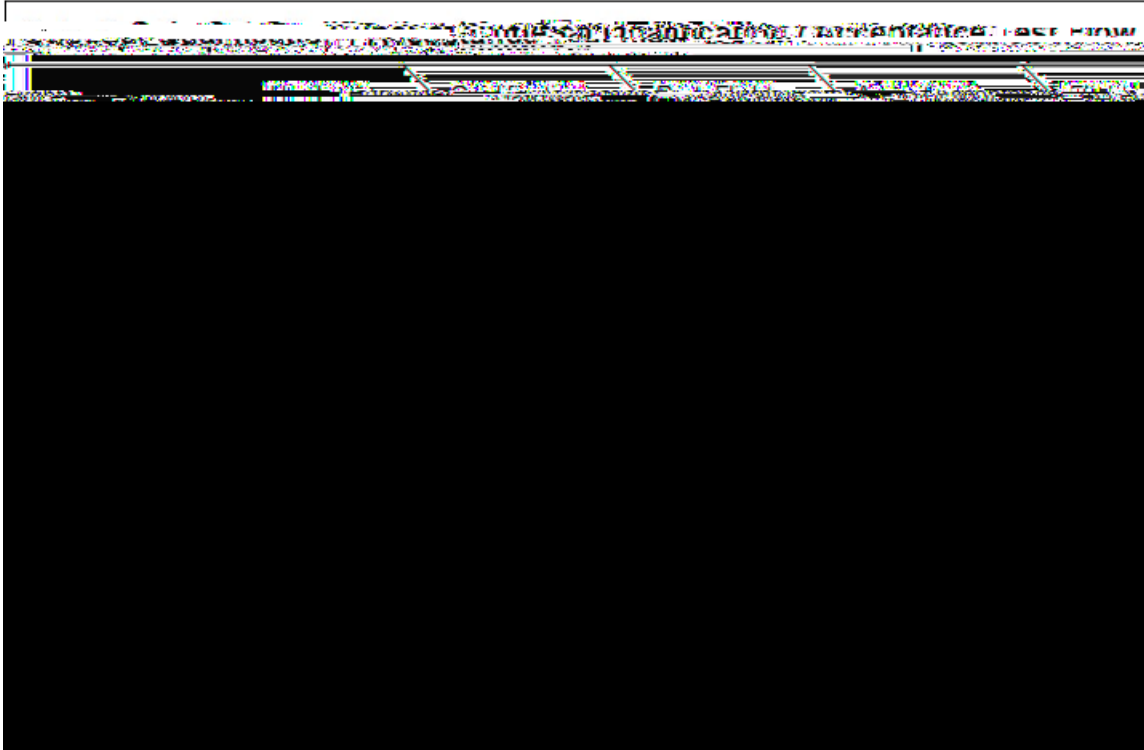


Figure 3.2 – CubeSat General Testing Flow Diagram [18].

The qualification testing is performed on a unit that is identical to the flight model CubeSat which would be APIS and this determines the Mission Integrator. The flight model is assessed at the acceptance levels in a Test 6U Dispenser. It will then be integrated into the flight 6U dispenser for a random vibration test as the final verification. There may be additional testing necessary if changes or modifications are made to the CubeSat after qualification testing.

The protoflight testing is only applied to the flight model CubeSat. This model is assessed at protoflight levels in a Test 6U Dispenser and then integrated into the flight 6U dispenser for a random vibration test that is the final verification. The flight CubeSat cannot be taken apart or modified at all after the protoflight test. If there is a modification, then the Mission Integrator is informed and determines the next steps.

4. Communication

4.1 Antenna

The antenna system will be located in the top two compartments of APIS with a total of four wire antennas that will be deployed on each side of APIS. The antenna will be equipped with a VHF/UHF (Very High Frequency/ Ultra-High Frequency) receiver whose frequency bands are 30-300 MHz and 300-1000 MHz respectively. Figure 4.1 shows the location of the four antennas when they will be fully deployed. The antenna extended shown in black in Figure 4.1 is a tape spring that is originally rolled up during launch shown in Figure 4.2. Each four of the antennas will be deployed at the same time so that the force exerted from the release of the tape spring will cancel each other out. The antenna wire is embedded within the tape spring to allow the antenna to easily deploy when necessary.

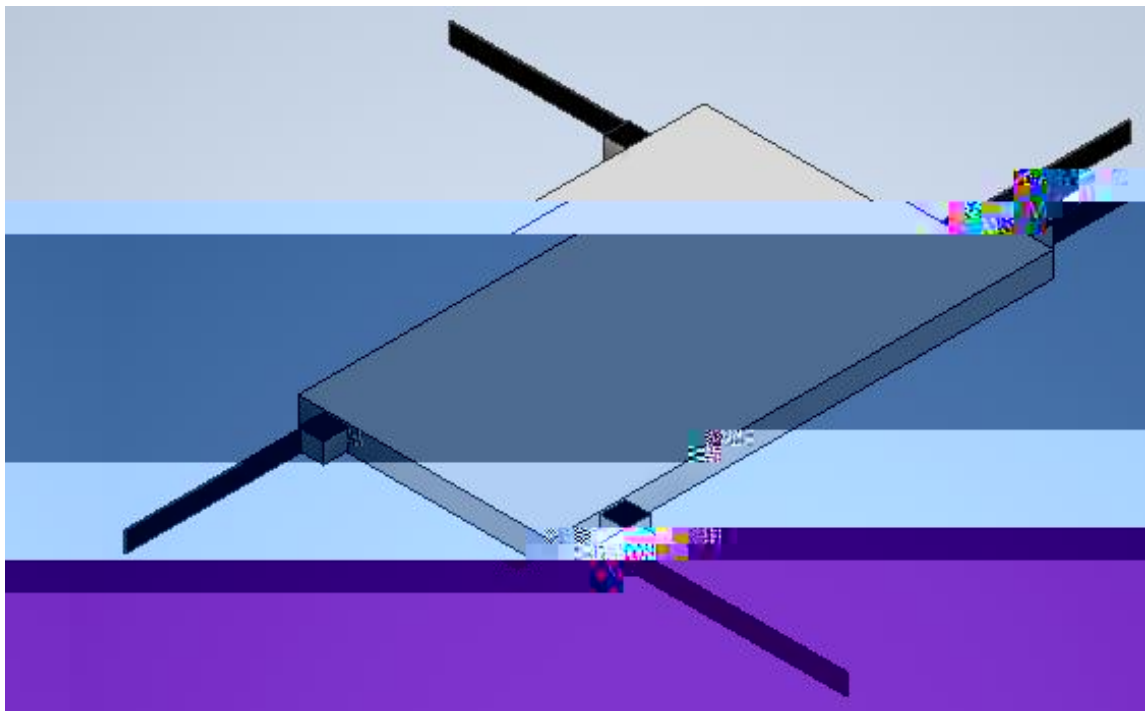


Figure 4.1 – Layout of four wire antennas.

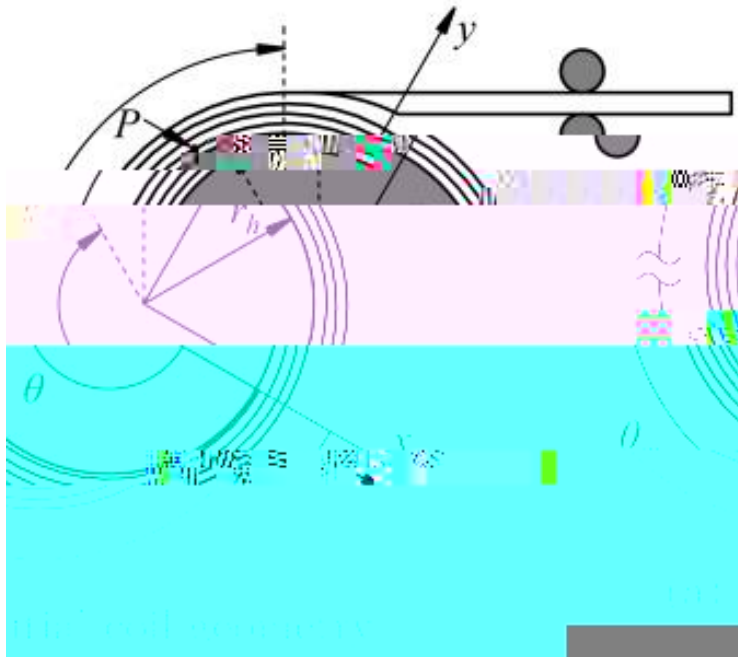


Figure 4.2 – Tape spring rolled up [19].

The mission requirements for an antenna as written by journal authors Sining Liu and coauthors should focus on telemetry, tracking and command, high-speed downlink for payload data, GPS and GNSS signal reception, and inter-satellite communication links [20]. These different requirements will change depending on the desired mission for the CubeSat but are achieved through this design with the VHF/UHF receiver that allows for reliable transmission and reception at the lowest possible volume.

5. Power System

5.1 Battery

CubeSats have two batteries: the primary battery and the secondary battery. The primary battery is non-rechargeable and is used in a one-time short use. It is normally used during or shortly after launch but can also be used over extended periods in short bursts. These batteries have a higher power density and a wider range of operating temperatures. The most common type of battery used within CubeSats is Lithium

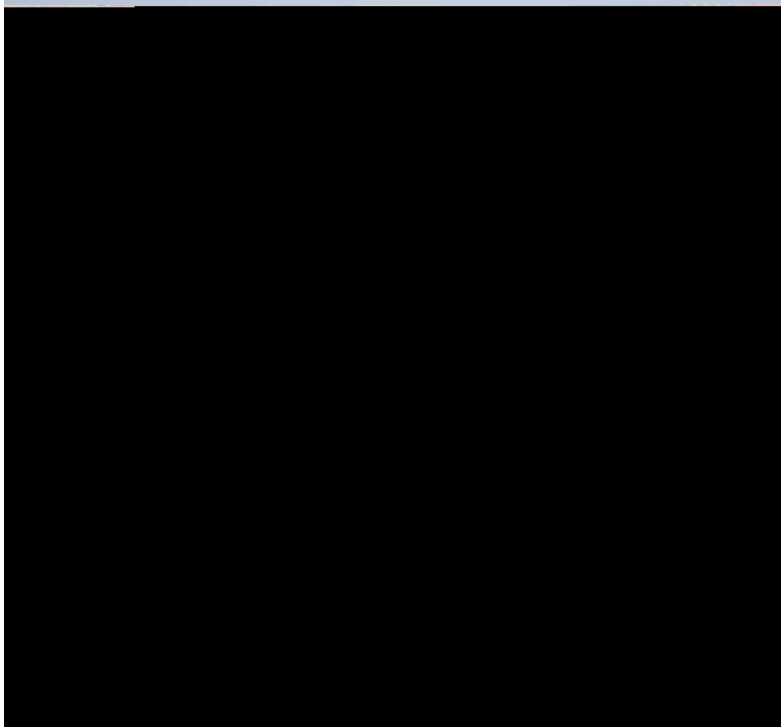


Figure 5.1 – Panels with solar panels.

6. Analysis

6.1 Finite Element Analysis

The Finite Element Analysis (FEA) within Inventor was utilized to predict how APIS will respond to the loads that it would experience during the launch.

$$= \tag{6.1}$$

The mass of the CubeSat structure is estimated to be around 2.388 kg (5.264 lb) from using the mass given by Inventor with the density of AlSi10Mg. The FEA will be completed with two pairs of load factors that are shown to be the extremes of what a payload aboard Falcon 9 rocket would experience. These two extreme pairs of load factors are 2 and 8.5 and 3 and 4 of the lateral and axial acceleration respectively. The forces that will be applied to APIS are calculated to be

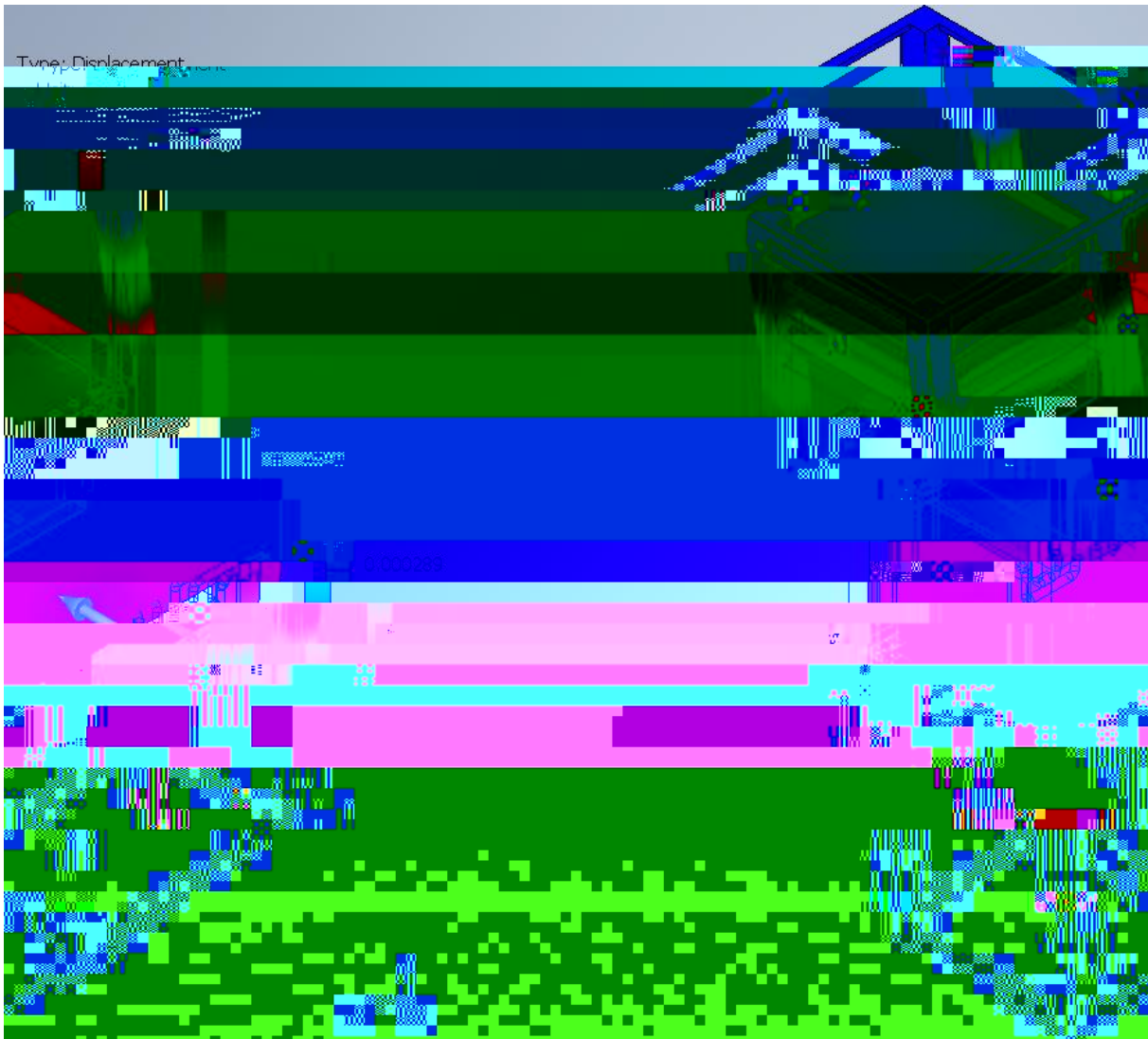


Figure 6.3 - Displacement for the second pair.

The displacement shown in Figure 6.2 has a max displacement of .00104 mm ($4.094E-5$ in) while Figure 6.3 has a max displacement of .001444 mm ($5.685E-5$ in). This difference shows that the face in the x-direction is more vulnerable to external forces during launch since the lateral acceleration force for the second pair is .5 times larger than the first pair while the axial force decreased by more than half from the first axial acceleration force to the second.

The safety factor for APIS was also calculated during the FEA in Inventor. Figures 6.4 and 6.5 show the safety factors calculated for both pairs. Both have the same safety factor of 15 across APIS. This high number shows that the structure is still viable even after the forces are applied to it. A lower number for the safety factor would mean that the structure is compromised and would not be reliable in the future.

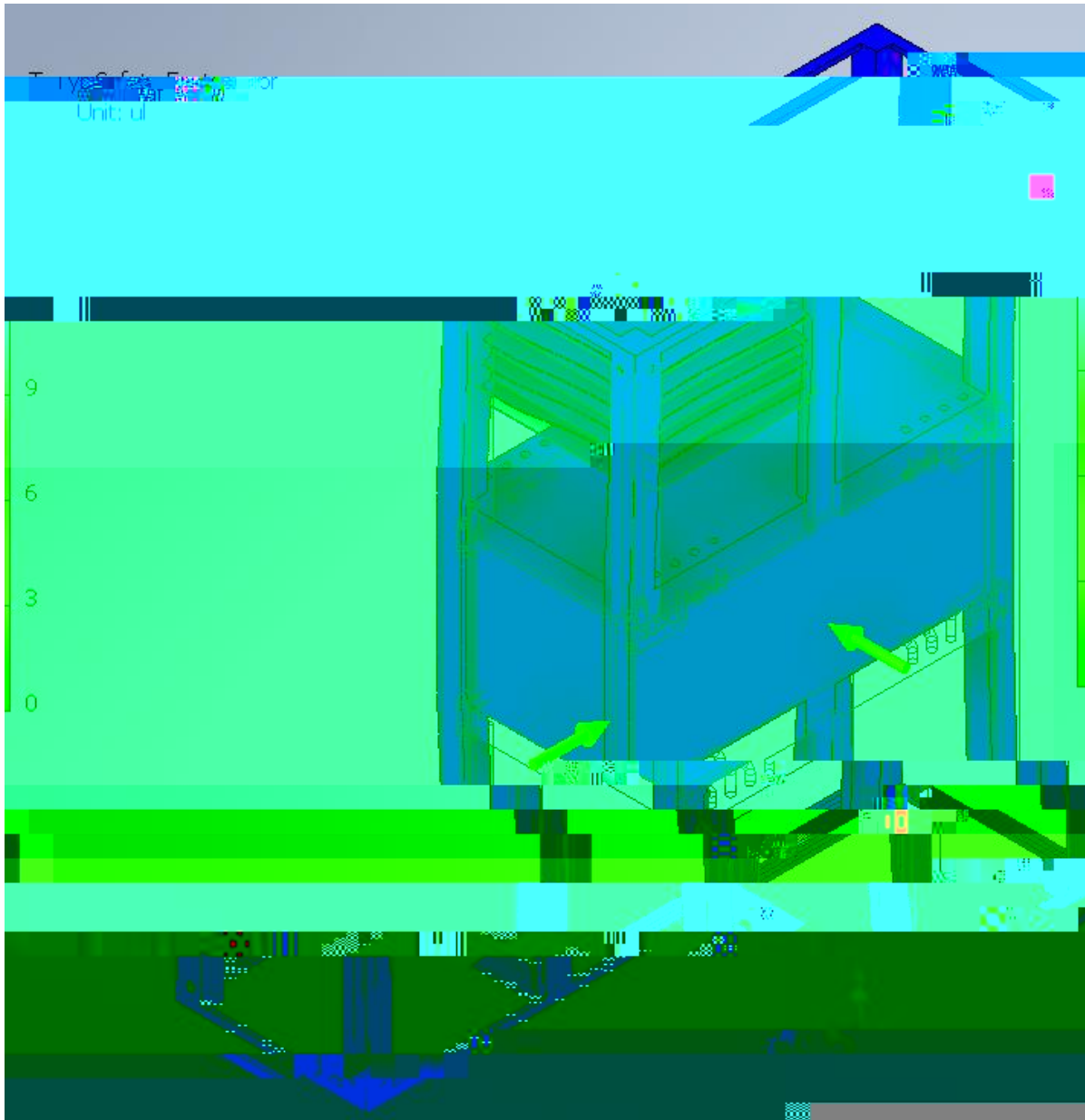


Figure 6.4 - Safety Factor for the first pair.

Figure 6.5 -

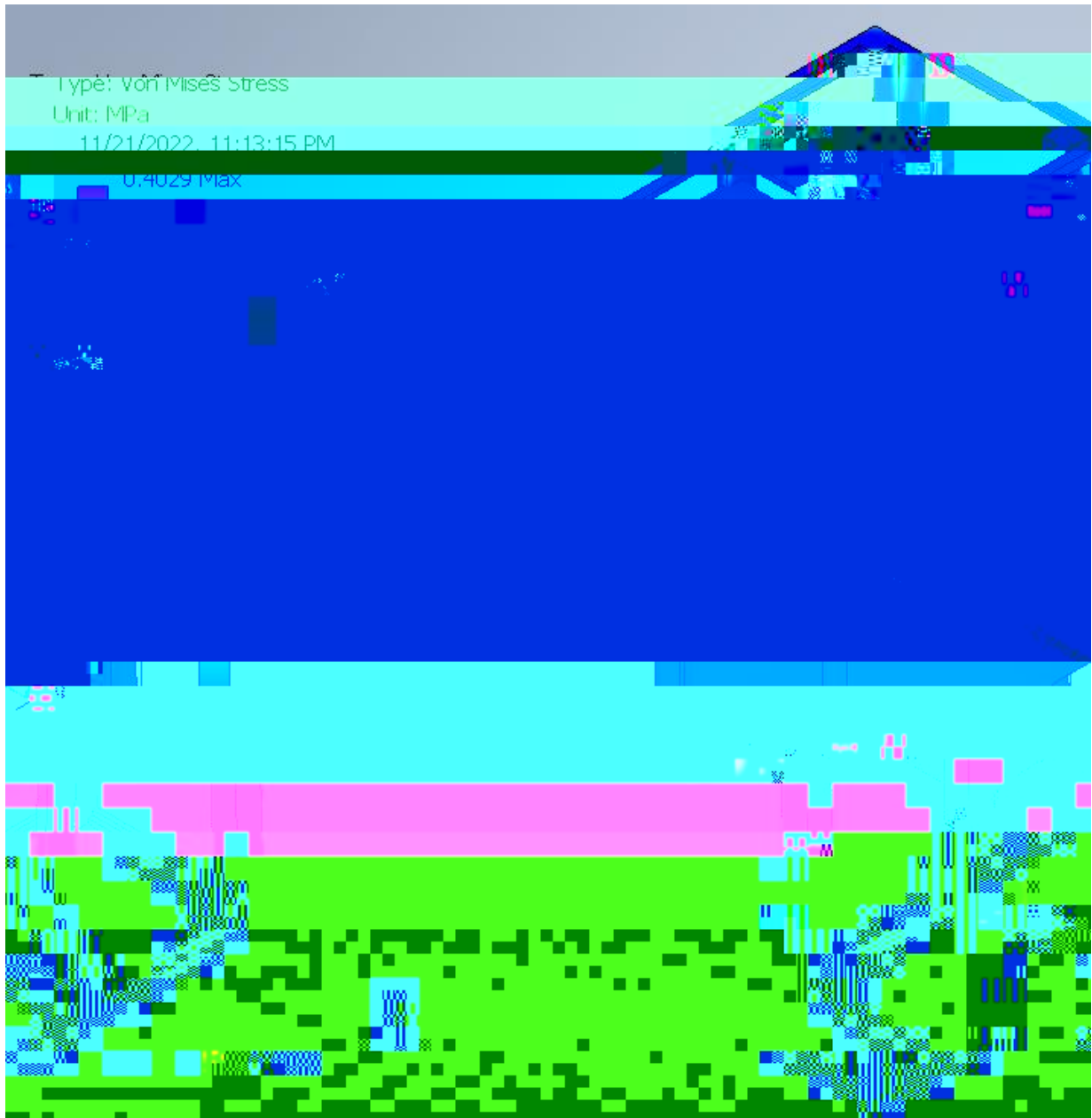


Figure 6.6 - Von Mises Stress for the first pair.

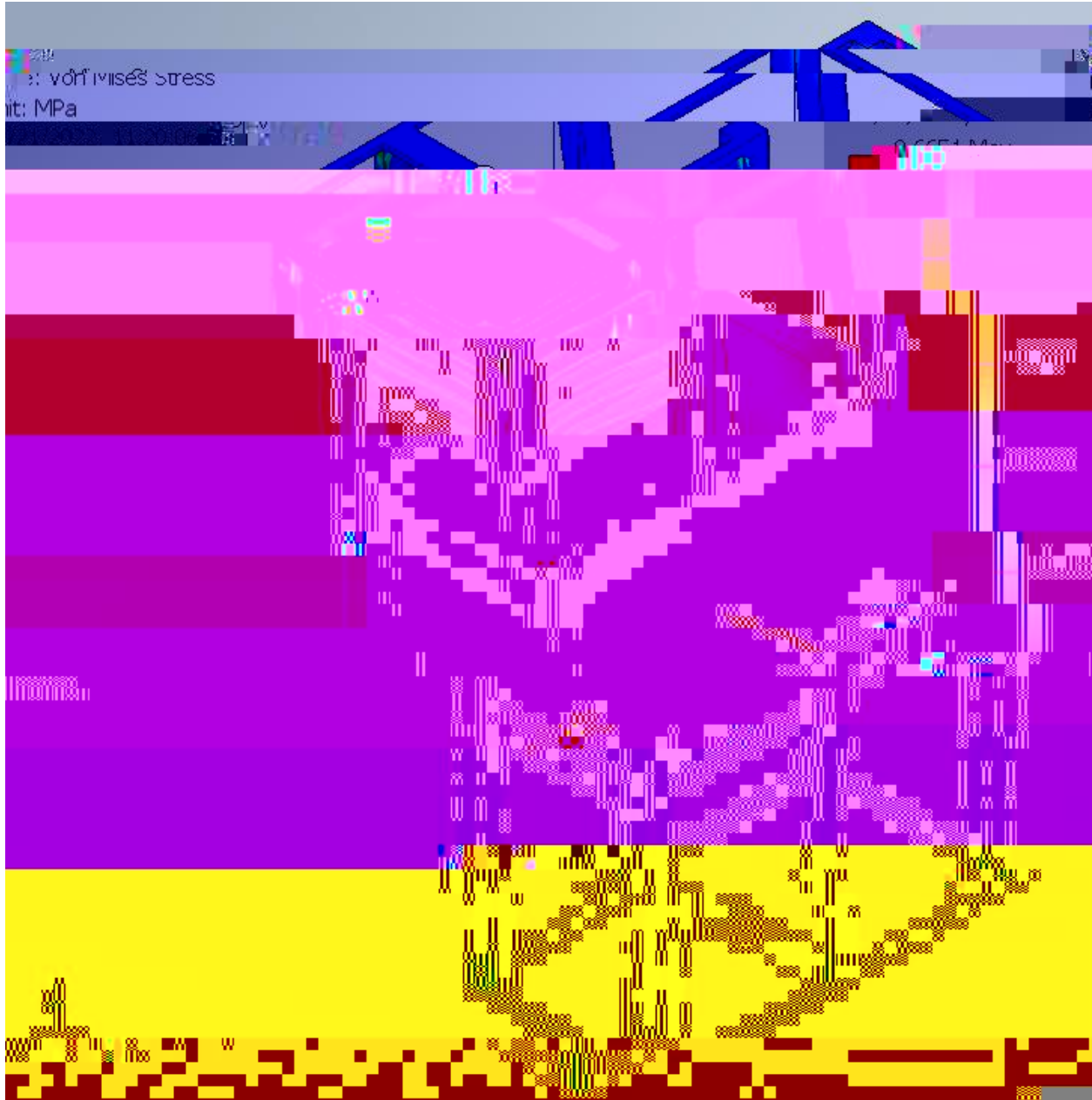


Figure 6.7 - Von Mises Stress for the second pair.

These analyses of the APIS structure demonstrate how it will still be functional and fully operational after it experiences the loads it would experience during the launch into space. This is especially necessary since if APIS got damaged during the launch, then it would be meaningless to launch it into orbit since it would not be able to complete its desired mission.

6.2 Thrust Analysis

The thrust force, shown in equation 6.2, will be calculated using a series of equations gathered from the NASA website [23]. Since APIS will be in Earth's orbit, the thrust can be

assumed to be in a vacuum, so the thrust equation becomes equation 6.3 where the pressure equations are ignored and the focus is on the exit velocity and the mass flow rate.

Thrust equation:

$$= \quad + \quad (\quad - \quad) \quad (6.2)$$

Thrust equation in a vacuum:

$$= \quad (6.3)$$

The exit velocity equation 6.5 is gathered from the exit Mach number equation shown in equation 6.5. The missing variables of exit Mach number and exit temperature are found in equations 6.6 and 6.9 respectively. The exit Mach number equation is derived by rearranging the area ratio in equation 6.7 and this derivation is shown in Appendix A.

Exit Velocity equation:

$$= \quad \underline{\hspace{2cm}} \quad (6.4)$$

Derived from the Mach number equation:

$$= \quad \underline{\underline{\hspace{2cm}}} \quad (6.5)$$

Exit Mach number equation:

$$= \left(1 + \frac{\left(\frac{\quad}{\quad} \right)^2 - 1}{2 \left(\frac{\quad}{\quad + 1} \right)} \right)$$

$$- = (1 +$$

References

- [1] Howell, E. (2018, June 19). *Cubesats: Tiny Payloads, huge benefits for space research.*

- [10] Loughborough University. (n.d.). *Sheet Lamination: Additive Manufacturing Research Group*. Loughborough University. Retrieved February 23, 2022, from <https://www.lboro.ac.uk/research/amrg/about/the7categoriesofadditivemanufacturing/sheetlamination/>
- [11] Loughborough University. (n.d.). *VAT Photopolymerisation: Additive Manufacturing Research Group*. Loughborough University. Retrieved February 23, 2022, from <https://www.lboro.ac.uk/research/amrg/about/the7categoriesofadditivemanufacturing/vatphotopolymerisation/>
- [12] Atkins. (2019). Additively manufactured mirrors for CubeSats. *SPIE Digital Library*., 11116, 11116–1111616. <https://doi.org/10.1117/12.2528119>
- [13] Snell. (2020). An additive manufactured CubeSat mirror incorporating a novel circular lattice. *SPIE Digital Library*., 11451. <https://doi.org/10.1117/12.2562738>
- [14] Boschetto. (2019). Selective Laser Melting of a 1U CubeSat structure. Design for Additive Manufacturing and assembly. *Acta Astronautica*., 159, 377–384. <https://doi.org/10.1016/j.actaastro.2019.03.041>
- [15] Sanchez. (2018). 3D-Metal-Printed 60 GHz Offset Dual-Reflector Antenna with Integrated Conical Feed Horn and Circular-to-

Khan M., and Matekovits L., “A Survey on CubeSat Missions and Their Antenna Designs,” *Electronics*, Vol. 11, 2022. <https://doi.org/10.3390/electronics11132021>

[21] Knap, V., Vestergaard, L., and Stroe, D., “A Review of Battery Technology in CubeSats and Small Satellite Solutions”, *Energies*, Vol. 13, 2020. <https://doi.org/10.3390/en13164097>

[22] Falcon 9 User Manual “Falcon User’s Manual,”

Appendix A

$$\begin{aligned}
 - &= \left(\frac{+1}{2}\right)^{-\frac{+1}{2(-1)}} \frac{\left(1 + \frac{-1}{2}\right)^{2\frac{+1}{(-1)}}}{2} \\
 &= \frac{+1}{-1}
 \end{aligned}$$

$$- = \left(\frac{+1}{2}\right)^{-\frac{2}{2}} \frac{\left(1 + \frac{-1}{2}\right)^2}{2}$$

$$[(-)]^2 = \left\{ \frac{1 + \frac{-1}{2}}{\frac{+1}{2}} \right\}^2$$

$$[(-)]^2 = \left\{ \frac{\frac{2}{-1} + 2}{\frac{+1}{-1}} \right\}^2$$

$$[(-)]^2 = \left\{ \frac{\frac{2}{-1} + 2}{-1} \right\}^2$$

$$= \left(\frac{-}{-}\right)^2, = 2, = \frac{2}{-1} = \frac{-1}{-1}, = \frac{-1}{+1} = \frac{1}{-1}$$

$$+ = 1, = 1$$

$$= (+)$$

$$() = (+)$$

$$() = (+)^{-1} = (+)^{-1}$$

$$(0) =$$

$$(1) = (+) = 1$$

$$(1) = (+)^{-1} = 1$$

$$(\) = + + 2$$

$$(\) = + 2$$

$$+ (0) = =$$

$$(1) = + + = 1$$

$$(1) = + 2 = 1$$

$$= , = 1 - 2 , =$$

$$= + + 2$$

$$= + (1 - 2) + 2$$

$$2 + \left[\frac{1 - - 2}{\ } \right] + 1 = 0$$

$$= \frac{-1}{2}$$

$$2 - 2 (+ 1) + 1 = 0$$

$$= (1 +) - \overline{(1 +)^2 - (1$$

$$= 1 + \frac{(-)^2 - 1}{2 \left(\frac{2}{+1}\right)^{\frac{+1}{-1}}} - 1 + ($$

$$\left(\frac{2}{+1} \right) ($$